

Article

Not peer-reviewed version

Wind-Generated Wave Modeling for the Location of Cermin Beach in Pantai Cermin District, Serdang Bedagai Regency

Ahmad Mulia , [Iqbal Baihaqi](#) * , [Emma Bangun](#)

Posted Date: 14 July 2025

doi: 10.20944/preprints202507.1120.v1

Keywords: wind waves; windrose; Jonswap parameters; finite water depth; Sverdrup Munk Bretschneider; return period



Preprints.org is a free multidisciplinary platform providing preprint service that is dedicated to making early versions of research outputs permanently available and citable. Preprints posted at Preprints.org appear in Web of Science, Crossref, Google Scholar, Scilit, Europe PMC.

Copyright: This open access article is published under a Creative Commons CC BY 4.0 license, which permit the free download, distribution, and reuse, provided that the author and preprint are cited in any reuse.

Article

Wind-Generated Wave Modeling for the Location of Cermin Beach in Pantai Cermin District, Serdang Bedagai Regency

Ahmad Perwira Mulia, Iqbal Muhammad Baihaqi * and Emma Patricia Bangun

Departement of Civil Engineering, University of North Sumatra, Medan, Indonesia

* Correspondence: iqbalmuhammad@students.usu.ac.id

Abstract

Wind waves are generally considered to be surface gravity waves caused by wind and propagating under the restoring force of gravity. These waves have maximum particle motion right at the air-sea interface, the particle motion decreases rapidly with depth. They are distributed over most of the ocean, with long waves propagating faster than short waves. The research method used for this study is quantitative analysis, namely from secondary data (wind speed and direction data) in the Cermin Beach area using the JONSWAP Parameters, Finite Water Depth and Sverdrup Munk Bretschneider methods. From the analysis results using the Windrose diagram, the dominant wind direction is $345^{\circ}-15^{\circ}$ with a percentage of 21.03%. For the Jonswap Parameters method, the maximum wave height and period are 0.906 m and 9.911 seconds. In the Finite Water Depth method, the maximum wave height and period for a depth of 3 meters are 1.304 m and 4.785 seconds, while at a depth of 10 meters they are 2.048 m and 6.743 seconds. In the Sverdrup Munk Bretschneider method, the maximum wave height and period for incomplete waves (Fetch Limited) are 1.815 m and 5.653 seconds, while for full waves (Fully Developed) they are 1.857 m and 5.750 seconds. In the results of the wave statistical return period, the maximum height results that occurred in the 100-year return period were obtained at a height of 10,445 m using the Gumbel method calculation with wave data from the Finite Water Depth method at a depth of 10 meters.

Keywords: wind waves; windrose; Jonswap parameters; finite water depth; Sverdrup Munk Bretschneider; return period

1. Introduction

Of the various types of wave motions that may occur in the ocean, wind waves are among the most energetic and easily observed. Therefore, one of the most studied waves is wind waves. Wind waves are generally considered to be surface gravity waves caused by wind and propagating under the restoring force of gravity. These waves have a maximum particle motion right at the air-sea interface, the particle motion rapidly decreasing with depth. They are distributed over most of the ocean, with long waves propagating faster than short waves.

Therefore, the behavior of waves generated by wind must be recorded every day in order to obtain their characteristic forms which will be useful in the future, both in research and in planning coastal building construction.

2. Materials and Methods

2.1. Wind

Wind, by definition, is the movement of air (primarily horizontal) in response to differences in air pressure caused primarily by differences in heating and cooling [1].

Wind data can be obtained from the nearest meteorological station or from the nearest airport. The data obtained is usually classified so that further data processing can be simpler and in general the data is sorted based on the distribution of wind speed and direction, as well as its percentage or known as windrose which can be seen in Figure 1.

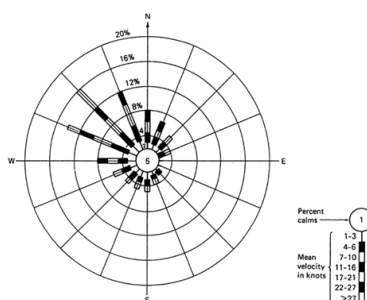


Figure 1. Windrose.

The wind speed in wave forecasting calculations must be the wind speed over water. In general, it is only necessary to know the wind speed from the nearest airport, and we must take into account that the wind over water is usually greater than the wind over land because of the smaller friction on the water. Therefore, a transformation of the wind data over land closest to the study location to the wind data over the sea surface is required.

The equation for wind speed that will be used for wave forecasting is:

$$U = R_T \cdot R_L (U_{10})_L \tag{1}$$

In this equation, R_T represents the correction factor accounting for temperature differences between the air and water, as illustrated in Figure 2. R_L denotes the correction applied to wind measurements taken on land, which is detailed in Figure 3. The term $(U_{10})_L$ refers to the wind speed measured at a height of 10 meters above ground level on land.

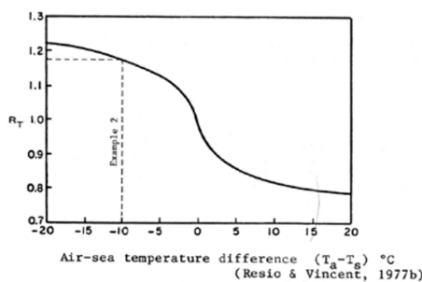


Figure 2. Speed correction coefficient for temperature difference (R_T).

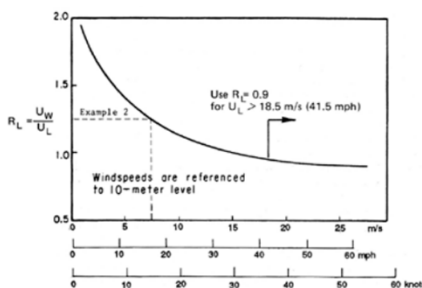


Figure 3. Correction coefficient for ground speed recording (R_L).

Correction between wind data on land and above sea level can use the following equation:

$$R_L = \frac{U_W}{U_L} \tag{2}$$

In this equation, the correction factor for wind speed on land, denoted as R_L , is used to adjust the wind speed measured above sea level (U_w) to its equivalent value over land (U_L). This factor accounts for the differences in surface roughness and friction between the sea and land surfaces, which affect wind speed. Specifically, R_L represents the ratio or relationship between the wind speed at sea and the wind speed observed over land, enabling more accurate assessments in meteorological and engineering applications.

The wind speed must be converted to the wind stress factor (U_A) using the following equation:

$$U_A = 0,71 U^{1,23} \quad (3)$$

In this equation, U represents the internal wind speed measured in meters per second. The variable U_A denotes the wind stress factor, which influences the value of the internal wind speed.

2.2. Fetch

In wave generation at sea, Fetch (which can be seen in Figure 4) is limited by the shape of the land surrounding the sea. In the wave formation area, waves are not only generated in the same direction as the wind direction but also at various angles to the wind direction [2]. For Fetch equation:

$$F_{eff} = \frac{\sum(X_i \cdot \cos a_i)}{\sum \cos a_i} \quad (4)$$

In this equation, F_{eff} represents the effective average fetch, which is a measure used to account for the varying distances over which wind blows across the water surface to generate waves. The term X_i refers to the length of each fetch segment, measured from the wave observation point to the end of the fetch in a specific direction. Meanwhile, a_i denotes the angular deviation on both sides of the primary wind direction, calculated using predetermined angle increments up to the maximum angle considered on either side of the wind direction.

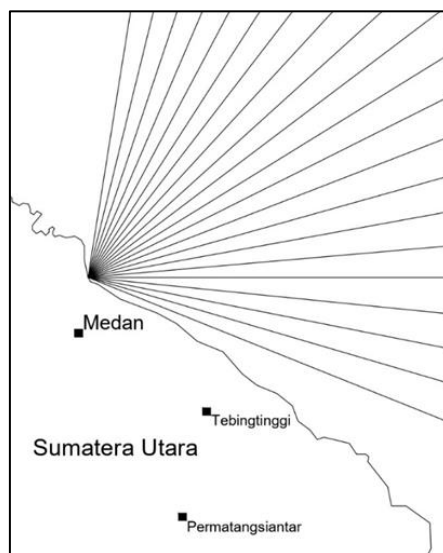


Figure 4. Example of Fetch depiction.

2.3. Wave

Waves in the sea can be divided into several types depending on the generating force. These waves are wind waves generated by wind blowing on the sea surface, tidal waves generated by the gravitational pull of celestial bodies, especially the sun and moon, tsunami waves caused by volcanic eruptions or earthquakes in the sea, waves generated by moving ships, and so on [2].

2.4. Jonswap Parameters

The Jonswap method for wave forecasting uses the following formula:

$$F^* = \frac{gF}{U^2}, H_{mo} = \frac{H_{mo}^* U^2}{g}, T_p = \frac{T_p^* U}{g}, t^* = \frac{gt}{U}, d^* = \frac{gd}{U^2} \quad (5)$$

Then, for the Jonswap relationship, namely:

$$H_{mo}^* = 0,0016(F^*)^{1/2} \quad (6)$$

$$T_p^* = 0,286(F^*)^{1/3} \quad (7)$$

$$F_{eff}^* = \left(\frac{t^*}{68,8}\right)^{\frac{3}{2}} \quad (8)$$

In this method, the dimensionless fetch length (F^*) is based on the actual fetch length (F) and is normalized with respect to wind conditions. The dimensionless zero moment wave height (H_{mo}^*) corresponds to zero moment wave height (H_{mo}), which represents the significant wave height derived from the wave energy spectrum. The dimensionless peak wave period (T_p^*) is derived from the peak wave period (T_p), the period associated with the peak energy in the wave spectrum. The dimensionless duration (t^*) is a scaled form of the actual duration (t) over which the wind acts. The dimensionless depth (d^*) represents the normalized value of the water depth (d). All these parameters are typically normalized using the wind speed (U), which plays a critical role in wave generation and growth. Additionally, the concept of effective fetch (F_{eff}^*) is used to represent a modified fetch that accounts for wind direction variability or other influencing factors, and is also expressed in dimensionless form. These dimensionless parameters allow for scalable, comparative analysis of wave characteristics across different oceanographic and meteorological scenarios.

2.5. Finite Water Depth

Water depth affects wave formation. For a given wind condition and fetch length, the wave height will be smaller and the wave period shorter if the formation occurs in transitional or shallow waters than in deep waters [3]. For the calculation, the following formula is used:

$$H^* = 0,24\{\tanh[0,53 \times d^*]\tanh[0,0125 \times F^*]\} \quad (9)$$

$$T^* = 7,54\{\tanh[0,83 \times d^*]\tanh[0,077 \times F^*]\} \quad (10)$$

In this method, several dimensionless parameters are used to describe wave characteristics. The dimensionless wave height is denoted by H^* , while the dimensionless wave period is represented by T^* . The dimensionless duration of wave generation is expressed as t^* , and the dimensionless depth of the water is indicated by d^* . These parameters are typically derived by normalizing their respective physical quantities with appropriate scaling factors, allowing for generalized analysis of wave behavior across different conditions.

2.6. Sverdrup Munk Bretschneider

The Sverdrup Munk Bretschneider (SMB) method is a method used to obtain significant sea wave height and period values. The SMB method calculation is formulated as follows:

2.6.1. Incomplete wave growth condition (Fetch Limited)

- Significant wave height (H_s);

$$\frac{gH_s}{U_A^2} = 1,6 \times 10^{-3} \left[\frac{gF}{U_A^2}\right]^{\frac{1}{2}} \quad (11)$$

- Significant wave period (T_m);

$$\frac{gTm}{U_A} = 2,857 \times 10^{-1} \left[\frac{gF}{U_A^2} \right]^{\frac{1}{3}} \quad (12)$$

$$Ts = 0,95.Tm$$

- Wind duration;

$$\frac{gt}{U_A} = 68,8 \left[\frac{gF}{U_A^2} \right]^{\frac{2}{3}} \quad (13)$$

2.6.2. Full wave growth conditions (Fully Developed)

- Significant wave height (H_s);

$$\frac{gH_s}{U_A^2} = 2,433 \times 10^{-1} \quad (14)$$

- Significant wave period (T_m);

$$\frac{gT_m}{U_A} = 8,134 \quad (15)$$

$$Ts = 0,95.Tm$$

- Wind duration;

$$\frac{gt}{U_A} = 7,15 \times 10^4 \quad (16)$$

In this method, H_s represents the significant wave height, which is a measure of the average height of the highest one-third of waves. T_m refers to the wave period, indicating the time interval between successive wave crests. The term F denotes the fetch length, which is the distance over water that the wind blows in a single direction. U_A is the wind stress factor, representing the influence of wind on the water surface. U stands for wind speed, while g is the gravitational acceleration, typically taken as 9.81 m/s^2 . T_s refers to the significant wave period, a specific measure related to H_s , and t indicates the duration for which the wind has been blowing over the fetch area.

2.7. Statistical Analysis of Waves

Long-term wave data analysis provides a theoretical distribution of the probability of occurrence of wave parameters over a number of years, this analysis is most often performed on long-term wave height data [4]. For calculations, it is done using the following equation:

- Normal Distribution;

$$P = \frac{1}{S_H \sqrt{2\pi}} \int_{-\infty}^H e^{-\frac{1}{2} \left(\frac{H - \bar{H}}{S_H} \right)^2} = \phi \left(\frac{H - \bar{H}}{S_H} \right) = \phi(Z) \quad (17)$$

$$Z = \frac{H - \bar{H}}{S_H} = \frac{1}{S_H} H - \frac{\bar{H}}{S_H} \quad (18)$$

$$A = \frac{1}{S_H}; B = -\frac{\bar{H}}{S_H} \quad (19)$$

$$\bar{H} = \frac{\sum(H \cdot N)}{\sum(N)} \quad (20)$$

$$H_{var} = \frac{\sum(N(H - \bar{H})^2)}{\sum(N)} \quad (21)$$

$$\sigma = \sqrt{H_{var}} \quad (22)$$

- Log-Normal Distribution;

$$Y = Z = \phi^{-1}P = \frac{\ln H - \overline{\ln H}}{S_{\ln H}} = \frac{1}{S_{\ln H}} \ln H - \frac{\overline{\ln H}}{S_{\ln H}} \quad (23)$$

$$X = \ln H; A = \frac{1}{S_{\ln H}}; B = -\frac{\overline{\ln H}}{S_{\ln H}} \quad (24)$$

- Gumbel Distribution;

$$Y = -\ln(\ln \frac{1}{P}) = G; X = H; A = \frac{1}{\beta}; B = -\frac{\gamma}{\beta} \quad (25)$$

- Weibull Distribution;

$$Y = \left(\ln \frac{1}{Q}\right)^{1/\alpha} = W; X = H; A = \frac{1}{\beta}; B = -\frac{\gamma}{\beta} \quad (26)$$

In this calculation of wave height analysis, the variable H represents the wave height, which is a key parameter in oceanographic and coastal studies. The symbol P denotes the probability associated with a specific wave height occurrence. σ stands for the standard deviation of wave height, reflecting the variability or dispersion of wave heights from the mean. Z refers to the standard normal variate, a dimensionless value derived from the standard normal distribution used in probabilistic calculations. \bar{H} indicates the mean wave height, which is the average value of all recorded wave heights. Lastly, H_{var} represents the variation or variance of wave height, quantifying the extent to which individual wave heights differ from the mean.

Then, to calculate the wave height with the return period for each distribution, the following equation is used:

- Normal Distribution;

$$H_{T_R} = \bar{H} + S_H \phi^{-1}(P) = \bar{H} + S_H \phi^{-1}\left(1 - \frac{1}{\lambda T_R}\right) \quad (27)$$

- Log-Normal Distribution;

$$\ln H_{T_R} = \overline{\ln H} + S_{\ln H} \phi^{-1}(P) = \overline{\ln H} + S_{\ln H} \phi^{-1}\left(1 - \frac{1}{\lambda T_R}\right) \quad (28)$$

- Gumbel Distribution;

$$H_{T_R} = \gamma - \beta \ln(\ln \frac{1}{P}) = \gamma - \beta \ln(\ln \frac{\lambda T_R}{\lambda T_R - 1}) \quad (29)$$

- Weibull Distribution;

$$H_{T_R} = \gamma + \beta \left(\ln \frac{1}{Q}\right)^{1/\alpha} = \gamma + \beta (\ln[\lambda T_R])^{1/\alpha} \quad (30)$$

In the given equation, H_{T_R} represents the wave height corresponding to a specific return period, T_R . The return period indicates the average time interval between occurrences of waves of a certain height or greater. \bar{H} denotes the mean wave height, while $S_{(\)}$ refers to the wave variance spectral density function, which characterizes the distribution of wave energy over frequencies. The symbol P stands for probability, often associated with the likelihood of exceeding a certain wave height. The parameters γ and β are shape and scale parameters, respectively, commonly used in Gumbel and Weibull distributions to statistically model extreme wave heights.

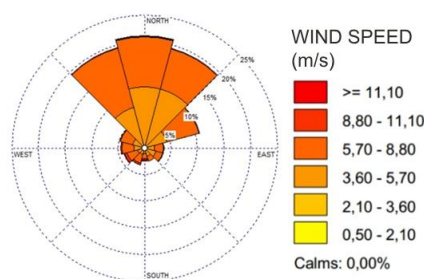
3. Results

3.1. Hydro-Oceanography Analysis (Wind)

The wind data used is the maximum daily wind speed and direction data from 2019 to 2023 obtained from the BMKG Kualanamu Meteorological Station. The wind data can be seen in Table 1 below. Furthermore, the wind data is displayed in the form of a Windrose diagram which can be seen in Figure 5.

Table 1. Wind Direction and Speed Table from 2019 to 2023.

Month	2019		2020		2021		2022		2023	
	Dir. (°)	Speed (m/s)								
January	237	6	286	6	173	5	215	6	229	6
February	223	6	213	6	290	6	223	6	237	5
March	271	7	272	6	201	6	207	7	195	6
April	232	6	179	6	133	6	278	6	223	6
May	227	6	170	5	142	6	140	5	148	6
June	141	6	130	6	177	5	130	5	112	6
July	138	5	125	6	116	6	143	6	112	6
August	129	6	102	6	130	5	138	6	175	6
September	170	6	127	5	133	6	141	6	150	6
October	172	5	135	5	167	6	154	5	213	5
November	210	5	206	5	258	6	241	5	286	5
December	291	5	299	5	310	6	222	5	255	5

**Figure 5.** Windrose Diagram on Cermin Beach from 2019 to 2023.

3.2. Fetch Length

The wind directions that affect this beach are Northwest, North, Northeast and East. In the Southeast direction it does not have a direct effect, but it allows for a deflection towards Pantai Cermin and affects the morphology of the beach. By drawing a long line from Pantai Cermin, the Fetch length with the Northwest, North, Northeast, East and Southeast generation areas. The Fetch length can be seen in Table 2.

Table 2. Table of Fetch Length on Cermin Beach.

α	Fetch Length (km)
120	456,93
114	292,66
108	257,73
102	261,31
96	238,35
90	223,13
84	198,4
78	195,63
72	191,24
66	194,21
60	205,1
54	216,41
48	214,85
42	227,14
36	222,21

30	296,43
24	316,48
18	296,39
12	324,52
6	317
0	455,65
-6	470,54
-12	587,69
-18	1000
-24	1000
-30	1000
-36	1000
-42	115,33

3.3. Determining Wave Height and Period

To forecast wave height, wind data is required which will then be processed using several deep sea wave forecasting equations, some of these equations are *Jonswap Parameters*, *Finite Water Depth* and *Sverdrup Munk Bretschneider*. The results of the calculations can be seen in Table 3, Table 4, Table 5, Table 6 and Table 7. The *Waverose* diagram can be seen in Figure 6, Figure 7, Figure 8, Figure 9 and Figure 10.

Table 3. Table of Wave Height and Period from 2019 to 2023 (*Jonswap Parameters*).

Month	2019		2020		2021		2022		2023	
	Height (m)	Period (s)								
January	0,687	8,981	0,646	8,801	0,586	8,513	0,642	8,785	0,653	8,802
February	0,686	8,995	0,662	8,895	0,707	9,075	0,703	9,064	0,632	8,754
March	0,754	9,279	0,735	9,195	0,720	9,129	0,765	9,317	0,691	9,004
April	0,690	8,988	0,648	8,824	0,656	8,846	0,725	9,049	0,698	9,051
May	0,668	8,819	0,627	8,717	0,706	9,051	0,631	8,713	0,728	9,118
June	0,660	8,828	0,644	8,768	0,633	8,741	0,594	8,576	0,660	8,871
July	0,597	8,570	0,679	8,925	0,672	8,899	0,661	8,890	0,638	8,766
August	0,638	8,745	0,646	8,807	0,594	8,544	0,683	8,947	0,646	8,802
September	0,702	8,939	0,606	8,571	0,717	9,054	0,656	8,844	0,656	8,844
October	0,582	8,478	0,594	8,543	0,679	8,948	0,631	8,706	0,582	8,488
November	0,582	8,510	0,629	8,711	0,683	8,943	0,609	8,640	0,625	8,692
December	0,594	8,558	0,601	8,590	0,661	8,880	0,582	8,484	0,605	8,630

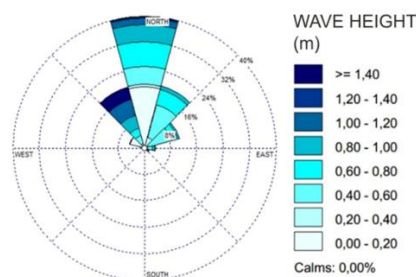


Figure 6. Waverose Chart from 2019 to 2023 (*Jonswap Parameters*).

Table 4. Table of Wave Height and Period from 2019 to 2023 (*Finite Water Depth, 3 meter*).

Month	2019	2020	2021	2022	2023
-------	------	------	------	------	------

	Height (m)	Period (s)								
January	1,133	4,374	1,253	4,680	1,546	5,406	1,264	4,702	1,316	4,825
February	1,087	4,288	1,162	4,508	1,040	4,114	1,033	4,150	1,300	4,869
March	0,872	3,631	0,950	3,878	0,986	3,913	0,853	3,610	1,086	4,230
April	1,130	4,321	1,222	4,634	1,229	4,633	1,157	4,448	1,032	4,133
May	1,346	4,743	1,345	4,947	1,091	4,221	1,389	5,083	1,049	4,163
June	1,324	4,839	1,360	4,955	1,323	4,914	1,454	5,276	1,191	4,568
July	1,483	5,263	1,199	4,549	1,226	4,610	1,167	4,558	1,318	4,896
August	1,357	4,932	1,255	4,735	1,511	5,339	1,185	4,542	1,267	4,732
September	1,310	4,591	1,493	5,247	1,156	4,311	1,249	4,700	1,246	4,681
October	1,594	5,468	1,466	5,212	1,155	4,454	1,362	4,880	1,567	5,434
November	1,540	5,459	1,359	4,942	1,179	4,418	1,391	5,059	1,377	4,972
December	1,484	5,275	1,456	5,191	1,188	4,546	1,548	5,405	1,409	5,168

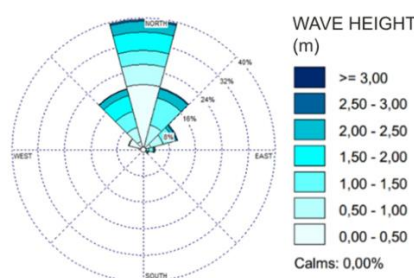


Figure 7. Waverose Chart from 2019 to 2023 (Finite Water Depth, 3 meter).

Table 5. Table of Wave Height and Period from 2019 to 2023 (Finite Water Depth, 10 meter).

Month	2019		2020		2021		2022		2023	
	Height (m)	Period (s)								
January	2,192	6,978	2,340	7,202	2,501	7,318	2,354	7,230	2,339	7,081
February	2,218	7,077	2,322	7,208	2,110	6,931	2,183	7,007	2,419	7,283
March	1,930	6,722	2,025	6,778	2,042	6,887	1,959	6,709	2,174	7,023
April	2,154	6,930	2,356	7,250	2,308	7,138	2,251	6,951	2,174	7,050
May	2,219	6,851	2,410	7,241	2,116	6,879	2,451	7,200	2,175	6,922
June	2,283	6,951	2,338	7,042	2,421	7,231	2,554	7,408	2,328	7,171
July	2,486	7,312	2,272	7,004	2,267	7,023	2,351	7,211	2,385	7,179
August	2,363	7,124	2,360	7,196	2,516	7,298	2,274	6,995	2,341	7,181
September	2,089	6,586	2,458	7,217	2,094	6,703	2,304	7,103	2,309	7,121
October	2,484	7,264	2,494	7,340	2,260	7,052	2,347	7,142	2,510	7,313
November	2,559	7,375	2,390	7,191	2,186	6,971	2,479	7,353	2,381	7,198
December	2,507	7,356	2,475	7,326	2,303	7,179	2,508	7,322	2,521	7,388

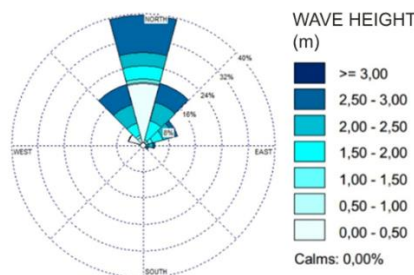
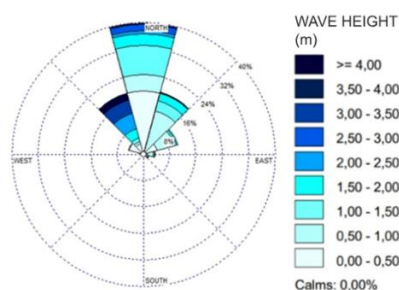


Figure 8. Waverose Chart from 2019 to 2023 (Finite Water Depth, 10 meter).

Table 6. Table of Wave Height and Period from 2019 to 2023 (*Sverdrup Munk Bretschneider, Fetch Limited*).

Month	2019		2020		2021		2022		2023	
	Height (m)	Period (s)								
January	1,327	2,837	1,527	3,745	1,858	4,985	1,543	3,814	1,561	3,801
February	1,268	2,576	1,341	2,805	1,237	2,540	1,206	2,355	1,488	3,326
March	1,071	2,013	1,134	2,174	1,237	2,718	1,032	1,828	1,320	2,934
April	1,374	3,166	1,452	3,340	1,462	3,405	1,332	2,830	1,215	2,404
May	1,746	4,967	1,583	3,815	1,296	2,787	1,581	3,682	1,224	2,454
June	1,537	3,632	1,571	3,724	1,546	3,654	1,683	4,113	1,407	3,160
July	1,781	4,678	1,421	3,261	1,426	3,196	1,328	2,705	1,511	3,439
August	1,609	3,976	1,476	3,404	1,836	4,961	1,361	2,912	1,502	3,543
September	1,692	4,770	1,985	6,458	1,417	3,424	1,444	3,223	1,446	3,247
October	1,965	5,545	1,972	6,420	1,342	2,858	1,738	4,805	1,922	5,342
November	1,790	4,553	1,646	4,200	1,441	3,448	1,673	4,249	1,674	4,323
December	1,781	4,665	1,755	4,590	1,382	2,993	2,036	6,580	1,599	3,703

**Figure 9.** Waverose Chart from 2019 to 2023 (*Sverdrup Munk Bretschneider, Fetch Limited*).**Table 7.** Table of Wave Height and Period from 2019 to 2023 (*Sverdrup Munk Bretschneider, Fully Developed*).

Month	2019		2020		2021		2022		2023	
	Height (m)	Period (s)								
January	1,092	5,036	0,924	4,664	0,744	4,145	0,909	4,630	1,053	4,759
February	1,054	5,016	0,959	4,800	1,150	5,209	1,132	5,168	0,863	4,537
March	1,335	5,636	1,276	5,471	1,205	5,335	1,439	5,750	1,086	5,063
April	1,116	5,073	0,913	4,676	0,966	4,754	1,857	5,492	1,093	5,122
May	1,191	4,925	0,865	4,499	1,192	5,212	0,959	4,553	1,494	5,453
June	1,066	4,817	0,987	4,671	0,894	4,550	0,733	4,199	0,969	4,783
July	0,774	4,241	1,142	4,989	1,087	4,916	0,956	4,785	0,916	4,602
August	0,958	4,616	0,922	4,662	0,784	4,215	1,152	5,020	0,928	4,665
September	1,393	5,253	0,880	4,341	1,366	5,359	0,974	4,756	0,974	4,756
October	0,758	4,123	0,763	4,211	1,074	4,970	0,915	4,549	0,742	4,117
November	0,716	4,105	0,893	4,522	1,114	5,012	0,792	4,339	0,876	4,488
December	0,752	4,204	0,779	4,271	0,964	4,790	0,740	4,118	0,764	4,291

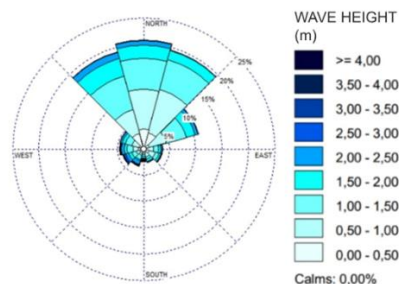


Figure 10. Waverose Chart from 2019 to 2023 (*Sverdrup Munk Bretschneider, Fully Developed*).

3.4. Statistical Analysis of Waves

The results of the statistical analysis of the calculation of the wave recurrence period using the method of Normal Distribution, Log-Normal Distribution, Gumbel Distribution and Weibull Distribution which show the largest wave height in each equation can be seen in Table 8, Table 9, Table 10, Table 11 and Table 12.

Table 8. Return Period with Weibull Distribution (*Jonswap Parameters*).

Ht	λ	α	β	Υ	Return Period (Year)		
					20	50	100
0,5	209,75	1,3	0,358	0,541	2,838	3,091	3,282
1	51	1	0,387	0,837	3,521	3,876	4,144
1,5	5,75	1,1	0,670	0,956	3,845	4,403	4,825

Table 9. Return Period with Gumbel Distribution (*Finite Water Depth, 3 Meter*).

Ht	λ	β	Υ	Return Period (Year)		
				20	50	100
0,5	300	0,408	1,037	4,587	4,961	5,244
1	195,5	0,271	1,419	3,661	3,909	4,097
1,5	77	0,195	1,893	3,327	3,506	3,641

Table 10. Return Period with Gumbel Distribution (*Finite Water Depth, 10 Meter*).

Ht	λ	β	Υ	Return Period (Year)		
				20	50	100
0,5	343,5	0,818	1,904	9,129	9,878	10,445
1	318,5	0,512	1,979	6,462	6,931	7,286
1,5	285,75	0,390	2,142	5,519	5,876	6,147

Table 11. Return Period with Weibull Distribution (*Sverdrup Munk Bretschneider, Fetch Limited*).

Ht	λ	α	β	Υ	Return Period (Year)		
					20	50	100
0,5	247,75	1,3	0,747	0,689	5,581	6,108	6,507
1	125,5	1	0,700	1,189	6,672	7,313	7,799
1,5	72,75	1,1	0,676	1,514	5,987	6,550	6,976

Table 12. Return Period with Weibull Distribution (*Sverdrup Munk Bretschneider, Fully Developed*).

Ht	λ	α	β	Υ	Return Period (Year)		
					20	50	100
0,5	365,25	1,3	0,574	0,622	4,551	4,956	5,262
1	221,75	1	0,668	0,688	6,301	6,913	7,377

1,5	31,25	1,1	0,624	1,750	5,400	5,919	6,312
-----	-------	-----	-------	-------	-------	-------	-------

4. Discussion

Based on the analysis of wind speed and direction data, the dominant wind direction at Cermin Beach is from 345° to 15° (North), with a frequency of 21.03%. Using the Jonswap Parameters method, the highest wave height and period were observed in March 2020, reaching 0.906 meters and 9.911 seconds. The Finite Water Depth method showed maximum wave characteristics in October 2023 with a wave height of 1.304 meters and period of 4.785 seconds at a depth of 3 meters, and in April 2022 with a height of 2.048 meters and period of 6.743 seconds at a depth of 10 meters. Meanwhile, the Sverdrup Munk Bretschneider (SMB) method recorded the highest wave height and period in non-full wave conditions in October 2019 (1.815 m, 5.653 s), and in full wave conditions, the highest wave height occurred in April 2022 (1.857 m), with the longest period in March 2022 (5.750 s).

For the 100-year return period analysis, the Jonswap Parameters method estimated a maximum wave height of 4.825 meters using the Weibull Distribution. The Finite Water Depth method predicted 100-year maximum wave heights of 5.244 meters at a depth of 3 meters and 10.445 meters at a depth of 10 meters using the Gumbel Distribution. The SMB method estimated maximum wave heights of 7.799 meters under incomplete wave conditions and 7.377 meters under full wave conditions, both using the Weibull Distribution. From these results, it can be concluded that the Jonswap Parameters method is the most suitable for wave forecasting at Cermin Beach, as the wave heights in the area are not categorized as extreme.

5. Conclusions

To obtain more accurate calculation results in future research, further analysis using a larger dataset is recommended, particularly by processing hourly wind data. Additionally, it is suggested to compare the analysis results using various methods, such as by employing wave forecasting models developed by institutions like BMKG or another institution, to enhance the reliability and validity of the findings.

Author Contributions: Conceptualization, A.P.M. and I.M.B.; methodology, A.P.M.; software, E.P.B.; validation, A.P.M. and E.P.B.; formal analysis, A.P.M.; investigation, I.M.B.; resources, A.P.M.; data curation, I.M.B.; writing—original draft preparation, I.M.B.; writing—review and editing, I.M.B. and E.P.B.; visualization, I.M.B.; supervision, A.P.M.; project administration, A.P.M.; funding acquisition, A.P.M. All authors have read and agreed to the published version of the manuscript.

Funding: This research received no external funding

Institutional Review Board Statement: Not applicable

Informed Consent Statement: Not applicable

Data Availability Statement: The wind direction and speed data presented in the study are obtained from Meteorology, Climatology and Geophysics Agency (BMKG), Indonesia. (requested on 10 June 2024)

Conflicts of Interest: The authors declare no conflicts of interest.

References

1. Tsinker, G. *Handbook of Port and Harbor Engineering*, 1st ed.; Springer New York: N.Y., United States of America, 1997.
2. Triatmodjo, B. *Teknik Pantai*, 5th ed.; Beta Offset: Yogyakarta, Indonesia, 1999.
3. Coastal Engineering Research Center. *Shore Protection Manual*, 4th ed.; US Army Corps of Engineers: Washington DC, United States of America, 1984.
4. Kamphuis, J. *Introduction to Coastal Engineering and Management*, 1st ed.; World Scientific: Farrer Road, Singapore, 2000.

5. Annenkov, S. Y., & Shrira, V. I. Evaluation of Skewness and Kurtosis of Wind Waves Parameterized by JONSWAP Spectra. *Journal of Physical Oceanography* **2014**, *44*, 1582–1594.
6. Applequist, S. Wind Rose Bias Correction. *Journal of Applied Meteorology and Climatology* **2012**, *51*, 1305–1309.
7. Chow, V. Te, Maidment, D. R., Mays. *Applied Hydrology*, Int. ed.; McGraw-Hill, Inc.: Texas, United States of America, 1988; pp. 1–294.
8. Fedorov, A. V., & Melville, W. K. A Model of Strongly Forced Wind Waves. *Journal of Physical Oceanography* **2009**, *39*, 2502–2522.
9. Gang, C., & Belcher, S. E. Effects of Long Waves on Wind-Generated Waves. *Journal of Physical Oceanography* **1999**, *30*, 2246–2256.
10. Huddiankuwera, A. Deformasi Gelombang pada Pemecah Gelombang Sisi Miring Berongga. Dissertation, Universitas Hasanuddin, Makassar, 21 December 2022.
11. Janseen, P. A. E. M. Wave-Induced Stress and the Drag of Air Flow over Sea Waves. *Journal of Physical Oceanography* **1989**, *19*, 745–754.
12. Lamont-Smith, T., & Waseda, T. Wind Wave Growth at Short Fetch. *Journal of Physical Oceanography* **2008**, *38*, 1597–1606.
13. Poddaeva, O., & Fedosova, A. Extreme Wind Speeds Analysis Using Extended Wind Rose Based on Statistic Methods. *Energy Reports* **2022**, *8*, 1177–1184.
14. Pratama, A. (2018). Analisa Statistik Gelombang yang Dibangkitkan di Wilayah Pantai Cermin. Undergraduate Thesis, Universitas Sumatera Utara, Medan, April 2018.
15. Purwanto, Tristanto, R., Handoyo, G., Trenggono, M., & Suryoputro, A. A. D. Analisis Peramalan dan Periode Ulang Gelombang di Perairan Bagian Timur Pulau Lirang, Maluku Barat Daya. *Indonesian Journal of Oceanography* **2020**, *2*, 80-89.
16. Raihan, G., Siregar, S., Adiningsih, S., & Heryanto, Y. Easywave untuk Peramalan Data Gelombang Laut Berbasis Pemograman Python Dengan Metode Sverrup, Munk and Bretschneider (SMB) (Studi Kasus: Perairan Sungairaden, Kalimantan Timur). *Jurnal Meteorologi Klimatologi Dan Geofisika* **2020**, *7*, 20-29.
17. Setiawan, E., Adrianto, D., Dharma, C. S., & Kurniawan, E. S. Pengolahan Gelombang Permukaan Laut Menggunakan Metode Sverdrup Munk Bretschneider (SMB) di Perairan Pulau Pabelokan. *Jurnal HIDROPILAR* **2016**, *2*, 133-146.
18. Shemdin, O. H. Wind-Generated Current and Phase Speed of Wind Waves. *Journal of Physical Oceanography* **1972**, *2*, 411–419.
19. Shilo, E., Ashkenazy, Y., Rimmer, A., Assouline, S., & Mahrer, Y. Wind Spatial Variability and Topographic Wave Frequency. *Journal of Physical Oceanography* **2008**, *38*, 2085–2096.
20. Sorensen, R. M. *Basic Coastal Engineering*, 2nd ed.; Springer New York: N.Y., United States of America, 1997; pp. 9-52.
21. Wright, J. W. The Wind Drift and Wave Breaking. *Journal of Physical Oceanography* **1976**, *6*, 402–405.

Disclaimer/Publisher's Note: The statements, opinions and data contained in all publications are solely those of the individual author(s) and contributor(s) and not of MDPI and/or the editor(s). MDPI and/or the editor(s) disclaim responsibility for any injury to people or property resulting from any ideas, methods, instructions or products referred to in the content.